Loop parametric scattering of cavity polaritons

S. S. Gavrilov

Institute of Solid State Physics RAS, 142432 Chernogolovka, Russia
and National Research University Higher School of Economics, 101000 Moscow, Russia

Within the framework of the mean-field approximation, a coherently excited two-dimensional system of weakly repulsive bosons is predicted to show a giant loop scattering when the rotational symmetry is reduced. The considered process combines (i) the parametric decay of the driven condensate into different k states and (ii) their massive backscattering owing to spontaneous synchronization of several four-wave mixing channels. The hybridization of the direct and inverse scattering processes, which are different and thus do not balance each other, makes the condensate oscillate under constant one-mode excitation. In particular, the amplitude of a polariton condensate excited by a resonant electromagnetic wave in a uniform polygonal GaAs-based microcavity is expected to oscillate in the subterahertz frequency domain.

I. INTRODUCTION

Two-dimensional cavity polaritons are a result of exciton-photon coupling in layered heterostructures [1–3]. Being composite bosons, they exhibit two kinds of coherent states, one of which is similar to Bose-Einstein condensates (BECs) formed with decreasing temperature [4], whereas the other appears when a resonant electromagnetic wave excites polaritons directly [5]. Both kinds of coherent states are characterized by a mean-field amplitude $\psi(\mathbf{r}, t)$ obeying a generalized wave equation

$$i\hbar \frac{\partial \psi}{\partial t} = [E(\mathbf{r}, -i\hbar\nabla) - i\gamma + V\psi^*\psi]\psi + f(\mathbf{r}, t) \qquad (1)$$

(spin degrees of freedom are disregarded). If the pumping force f and decay rate γ are zero, Eq. (1) is reduced to the Gross-Pitaevskii equation for equilibrium BECs. Similar to atomic gases, cavity polaritons combine repulsive interaction ($V > 0$) and positive mass in the vicinity of the ground-state level $E_g = E(\mathbf{k} = 0)$ [2,3].

Under plane-wave pumping [e.g., $f(\mathbf{r}, t) = \bar{f}e^{i(\mathbf{k}_p\mathbf{r} - E_p t/\hbar)}$], the condensate has the same wave vector and frequency as the pump wave, provided that $\gamma > 0$ and E_p is not too far from resonance. The forced oscillation of ψ results in deep qualitative changes of the Bogolyubov excitation spectrum $\tilde{E}(\mathbf{k})$ compared with equilibrium systems [6,7]. In particular, the excitations around $\mathbf{k}_p = 0$ are no longer sonic unless E_p is equal to $E_g + V|\psi_{\mathbf{k}=0}(\bar{f})|^2$ for a given pump amplitude $\bar{f}$ [8]. Besides, as $\bar{f}$ and $|\psi_{\mathbf{k}_p}(\bar{f})|$ are increased, the sign of Im $\tilde{E}$ may reverse at some $\mathbf{k} = \mathbf{k}'$, which means the instability of the condensate against two-particle scattering $(\mathbf{k}_p, \mathbf{k}_p) \rightarrow (\mathbf{k}', 2\mathbf{k}_p - \mathbf{k}')$, often leading to a strong redistribution of polaritons in the $\mathbf{k}$ space. For instance, the breakup of the condensate excited with a nonzero $\mathbf{k}_p$ near the inflection point of $E(|\mathbf{k}|)$ is known to result in macroscopic occupation of two modes $\mathbf{k} \approx 0$ and $\mathbf{k} \approx 2\mathbf{k}_p$ [9–11]. Such processes, which

attracted much interest in the early 2000s, were firstly understood by analogy with optical parametric oscillators (OPOs) [12,13], in which an external pump beam splits into a pair of plane waves, conventionally referred to as "signal" and "idler." This analogy is not perfect because the polariton OPO arises through fluctuations [14] and never comes to a state with only three nonempty wave modes [15–17]. Nevertheless, the condensate induced by coherent pumping usually remains the most populated mode that governs all signals and idlers excited owing to the parametric scattering [18–21].

Here, we report an unusual manifestation of the parametric scattering, which is expected to occur in wide (tens of micrometers) and spatially uniform samples of a polygonal shape. We show that a reduced rotational symmetry leads to a sort of population inversion such that a number of scattered modes get noticeably stronger than the pumped mode ($\mathbf{k}_p = 0$, $E_p > E_g$). Consequently, new two-particle interaction processes come into play which are different from the direct breakup of a pumped condensate into signals and idlers; furthermore, the pumped mode can itself act as a parametric signal. By virtue of symmetry, several processes of such kind synchronize, share the same target state $\mathbf{k} = 0$, and thus yield a massive backscattering of polaritons. It is important that the direct and inverse scattering effects do not cancel each other but constitute a unified loop interaction process. The common signal of the backscattering arises near the ground-state energy level E_g rather than at the pump level E_p. As a result, the pumped mode has two energy peaks, and its amplitude $|\psi_{\mathbf{k}=0}|$ oscillates at frequency $\sim (E_p - E_g)/\hbar$. At the same time, several scattered modes with $\mathbf{k} \neq 0$ remain nearly steady and very strong, being thus a dynamical reservoir that feeds the new condensate.

In what follows, all these phenomena are considered in detail. We begin in Sec. II with describing the feedback between the externally pumped and scattered polariton modes which is responsible for their abnormal population. The same feedback
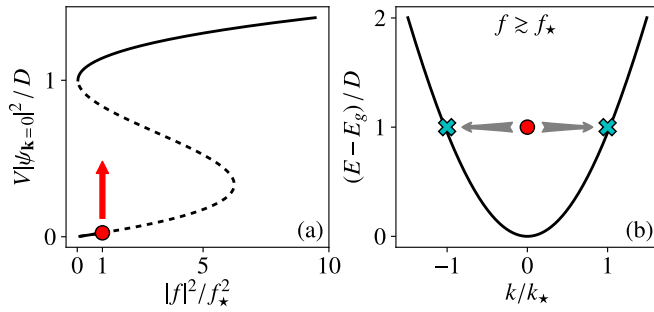
FIG. 1. (a) One-mode response of a driven condensate; the dashed line indicates unstable solutions; $D = E_p - E_g = 40\gamma$ is the pump detuning from the resonance at $\mathbf{k}_p = 0$; $f_\star = \sqrt{(\gamma/V)[(D-\gamma)^2 + \gamma^2]}$ [22]. (b) Dispersion law, position of the pumped mode, and scheme of the parametric scattering. The scattering wave number $k_\star \approx 0.9~\mu\mathrm{m}^{-1}$.

mechanism was found earlier in isotropic systems, both infinite [22,23] and strongly confined [24], where it had different observable manifestations. In Sec. III we demonstrate the onset of the macroscopic loop interaction in a square cavity. Finally, in Sec. IV, we summarize the results and compare them with some recent studies dealing with the dynamical condensation [25] and self-pulsations in a polariton fluid under coherent driving [26,27].

II. BLOWUP AND ABNORMAL POPULATION OF SCATTERED MODES

Let us recall several basic facts about an interplay between the parametric scattering and bistability in a homogeneous and isotropic polariton system. It is known that the one-mode dependence of $|\psi_{\mathbf{k}_p}|^2$ on $|f|^2$ has an "S"-shaped form [Fig. 1(a)] as long as $D \equiv E_p - E(\mathbf{k}_p) > \sqrt{3}\gamma$ [7,28–30]. When $|\psi_{\mathbf{k}_p}|$ is small, the repulsive interaction of polaritons ($V > 0$) involves a blueshift of their resonance energy $E(\mathbf{k}_p) + V|\psi_{\mathbf{k}_p}|^2$ towards the pump level E_p, resulting in a superlinear increase in $|\psi_{\mathbf{k}_p}|$ as a function of $|f|$ throughout the lower branch of solutions. On the upper branch, by contrast, the dependence of $|\psi_{\mathbf{k}_p}|$ on $|f|$ is sublinear, because the effective resonance energy has exceeded E_p and shifts still farther as $|f|$ increases. The segment with a negative slope consists of unstable solutions.

Notice that a sizable portion of the lower branch can also be unstable because of an intermode scattering [30] such as shown in Fig. 1(b) for the case of $\mathbf{k}_p = 0$. The imaginary part of the energy $\tilde{E}(\mathbf{k})$ of elementary excitations changes its sign for some $\mathbf{k} = \mathbf{k}_\star$ at a certain threshold point $|f| = f_\star$, resulting in a spontaneous growth of $|\psi_{\mathbf{k}_\star}|$. Specifically, this occurs when blueshift $V|\psi_{\mathbf{k}_p}|^2$ exceeds γ, whereas at the end of the lower branch of one-mode solutions the blueshift would have reached a much greater value of $D/3$ in the limit $\gamma/D \to 0$. Thus, in the case of small γ, one can estimate $\mathbf{k}_\star$ directly from an unshifted dispersion law $E(\mathbf{k})$ taking into account energy and momentum conservation [Fig. 1(b)]. If $\mathbf{k}_p = 0$, all $\mathbf{k}_\star$ lie on a ring-shaped intersection of the renormalized energy surface $\tilde{E}(\mathbf{k})$ and pump level $E = E_p$ [22].

Since the scattering threshold $f_\star$ is less than the bistability turning point, the question arises of what exactly happens to the system when the pump amplitude slightly exceeds $f_\star$. Proceeding from certain analogies in laser physics, one might expect a second-order phase transition with a continuous amplification of scattered modes upon increasing f, which is indeed quite a common behavior of dissipative systems in which $\max_{\mathbf{k}} \mathrm{Im}\, \tilde{E}(\mathbf{k})$ smoothly changes its sign in a critical point [31]. However, the answer is different and counterintuitive: The parametric breakup of the driven mode is accompanied by a growth rather than decrease of its own amplitude $|\psi_{\mathbf{k}_p}|$ [22]. This is possible despite the $|\psi|^4$ interaction being of the "conservative" kind, because the system is open. As a result, the total $|\psi|$ grows spontaneously even at constant $|f|$ until the blueshift cancels the pump detuning. Such a process shows a hyperbolic time dependence with a latency period that tends to infinity for $|f| \to f_\star + 0$ but otherwise ends up in a singularity point with a very sharp jump of the field. Analogous scenarios are known as regimes with blowup ([32]).

The scattering may lead to an unusual state in which population of scattered modes $I_s = \sum_{\mathbf{k} \neq \mathbf{k}_p} |\psi_{\mathbf{k}}|^2$ overcomes $I_p = |\psi_{\mathbf{k}_p}|^2$. When $D/\gamma \gtrsim 10$ and $|f|$ is close to the threshold, I_s can be several times greater than I_p during a short period just before the jump to the upper branch. In a uniform system, the growth of I_s results in the one-mode instability of the pumped mode (so that its lower-energy state disappears [22]); thus the value of I_s/I_p cannot be abnormally high for a long time. In the special case of $\mathbf{k}_p = 0$, the parametric scattering turns into a purely transient process that mediates the jump to the upper stability branch and, in particular, reduces the corresponding threshold at the cost of a potentially lengthy latency period.

The key idea of this work is that an abnormally high population of scattered modes (i.e., a sort of population inversion for the case of parametric scattering) can be stabilized owing to a reduced symmetry. Let us consider a square quantum well (mesa) with a side of $L \approx 40~\mu\mathrm{m}$ and indefinitely high energy barrier at the boundary. The main parameters are $\gamma = 0.01$ meV, $D = 0.4$ meV, and $\mathbf{k}_p = 0$; the exciton-photon detuning at $\mathbf{k} = 0$ is zero, and thus the polariton mass m is two times larger than the photon mass $m_{\mathrm{ph}} = \epsilon E_0/c^2$, where $E_0 = 1.5$ eV and $\epsilon = 12.5$ (as in typical GaAs-based microcavities). We took into account the nonparabolicity of $E(\mathbf{k})$, yet it does not play a significant role at small D. The interaction constant V only determines $f_\star \propto V^{-1/2}$ and can be chosen arbitrarily.

Figure 2(a) shows a steady-state dependence of an average $V|\psi|^2$ on $|f|^2$. Compared with Fig. 1(a), it contains three rather than two stability branches as well as several isolated points representing transient solutions. As expected, (i) the response is linear for $|f| \to 0$, and (ii) the uppermost branch is characterized by a fully canceled pump detuning ($V|\psi|^2/D \gtrsim 1$). This branch is reached at a relatively small pump power $|f|^2 \approx 0.5 f_\star^2$, which is not surprising since the presence of sharp potential walls involves the Rayleigh scattering into different k states with $\tilde{E}(\mathbf{k}) = E_p$; as a result, the polariton density $\langle|\psi|^2\rangle$ is higher than in a flat cavity at the same f unless the system has arrived at the upper branch where all scattering channels are closed. It is remarkable, however, that the response becomes nonlinear already at $V\langle|\psi|^2\rangle \lesssim 10^{-2}D$, i.e., far below the threshold value of $V\langle|\psi|^2\rangle$. This is
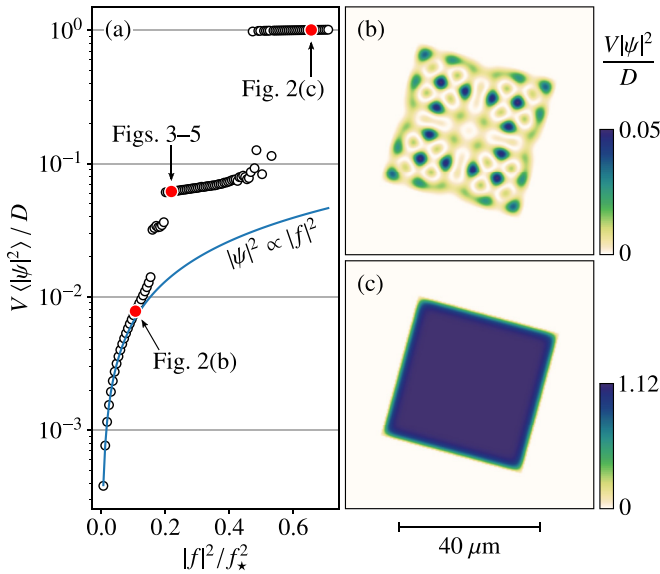
FIG. 2. (a) Steady-state response to excitation in a square microcavity mesa. Parameters are indicated in the main text. Circles represent independent solutions. Intensities $|\psi(\mathbf{r}, t)|^2$ are averaged in space (over the mesa) and time (over 0.1 ns) after a 1-ns-long period of increasing $|f|$ from zero to a given amplitude and an extra 2-ns-long period allotted for the establishment of a particular solution at a fixed $|f|$. (b) and (c) Explicit spatial dependences for two solutions.
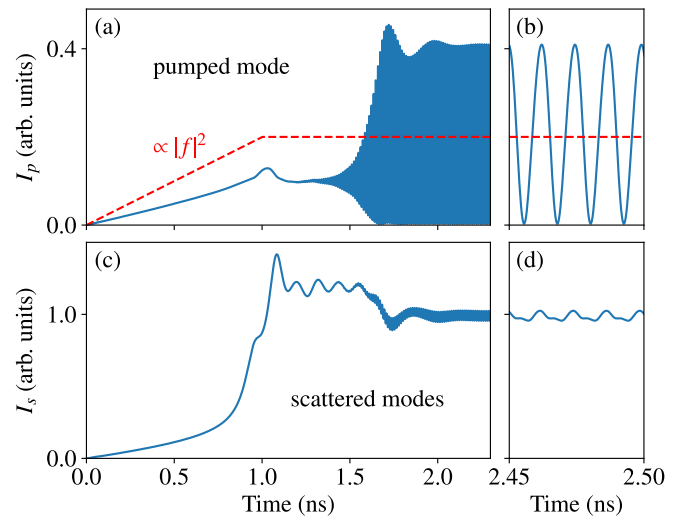

FIG. 3. Dynamics of the intensities of the pumped [(a) and (b)] and scattered [(c) and (d)] modes. The pump power $|f|^2$ is linearly increased in 1 ns from 0 to $\sim 0.22 f_\star^2$. (b) and (d) represent an established solution on a more detailed time scale.

explained by the fact that the field is strongly inhomogeneous even inside the mesa and has several short-range areas with comparatively high $|\psi|^2$. As seen in Fig. 2(b), the maximum $V|\psi|^2$ equals $0.05D = 2\gamma$, which is twice greater than the threshold, whereas the average $V|\psi|^2$ is still less than $0.008D$.

In turn, the strong inhomogeneity is explained by a reduced rotational symmetry, owing to which the Rayleigh scattering has certain preferred directions matching the system geometry. If a square mesa is oriented along the x and y axes, the preferred k states are $(\pm k_R, 0)$ and $(0, \pm k_R)$, where $k_R \approx \sqrt{2mD}/\hbar$. Indeed, the reflection of each of these waves from a potential wall yields a twin wave with the inverse $\mathbf{k}$, whereas all other waves would eventually scatter into many modes and lose coherence. The filling of the geometrically preferred states reveals itself in the formation of a semiperiodic standing-wave pattern whose sharpness appears to be as high as in Fig. 2(b) even at $|f| \to 0$. Since $k_\star = k_R$ for $k_p = 0$, the already dominant k states (filled via the Rayleigh scattering) and the corresponding real-space lattice get amplified parametrically upon increasing $|f|$. Thus the onset of the parametric scattering takes place in a number of small spots rather than in the whole system at once.

The short-range parametric instability has been studied earlier by focusing the pump into a 2-μm spot on the sample [24]. In that case, one could no longer distinguish the pumped and scattered k states and analyze their interaction in the spirit of Ref. [22]. Nonetheless, the bistability effect as well as thresholdlike parametric scattering were observed. It was found that, in contrast to the case of one-mode excitation, the onset of the instability does not end up with a jump to the

upper branch in a finite range of pump powers. The blowup remains unfinished, because the growth of $|\psi|$ at the spot center makes polaritons more intensively spread out of the parametrically unstable area, which is equivalent to additional energy losses. Such a system permanently remains in a state with many-mode instability; as a result, it exhibits strong quantum noise and spontaneous pattern formation [24].

The middle branch seen in Fig. 2(a) at $0.2 \lesssim |f|^2/f_\star^2 \lesssim 0.5$ has a similar nature. The collective states with strong parametric instability are stabilized on the average owing to additional losses. Considering the real space, one can say that polaritons ballistically move from the higher-energy "growth" areas to the "decay" areas. In the momentum space, the same process is seen as the scattering into a continuum of highly dissipative modes. The dominant k states suppress the field at the places of their negative interference, which makes the system inhomogeneous and prevents its continuous transition to the uppermost branch where the field is, by contrast, spatially uniform [Fig. 2(c)].

In summary, the Rayleigh scattering plays the role of a precursor to the parametric oscillation transition. As f is increased, the system becomes parametrically unstable within a number of spatially isolated areas where the field is the most strong. The instability results in a discontinuous transition accompanied by a sharp growth of the total intensity. However, the system remains strongly inhomogeneous and does not reach the upper branch of solutions in a wide range of f.

III. MACROSCOPIC LOOP INTERACTION

Let us now turn to a detailed analysis of one characteristic solution close to the beginning of the middle branch. Figure 3 explicitly shows the intensities of the pumped (I_p) and scattered (I_s) modes depending on time for $|f|^2/f_\star^2 \approx 0.22$. Technically speaking, I_p is summed over $k_{x,y} = 0 \pm 0.08 \, \mu\text{m}^{-1}$ in order to take account of mode broadening in
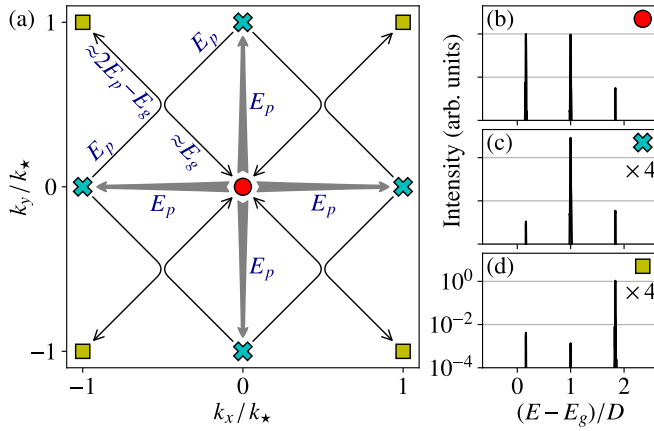
FIG. 4. (a) Scheme of the loop parametric scattering. (b)–(d) The spectra of the main k states at the stage of regular oscillations.

a confined system, and accordingly, I_s is summed over the rest of the k space.

The pump is turned on slowly (in 1 ns) to illustrate the onset of the instability. Initially, we have $I_p \propto |f|^2$ and $I_s \propto I_p$ (the Rayleigh scattering is linear). The increase in $|f|$ beyond the parametric threshold leads to a significant increase in I_s, which is typical of the first stage of blowup when much energy is transferred into the system of scattered modes whereas the pumped mode is increased only slightly [22]. As we have argued previously, this process does not involve the entire area of the mesa, and so the accumulated I_s is still insufficient for triggering a global one-mode instability of $\mathbf{k} = 0$. As a result, by $t \approx 1.1$ ns the system gets locked in a state with $I_s/I_p \gtrsim 10$.

Since the normal way out of the many-mode instability is unfeasible, qualitatively new collective phenomena come into being. In particular, the pumped mode exhibits self-pulsations whose amplitude rapidly grows in the interval from $t \approx 1.3$ ns to 1.7 ns, after which a fairly regular oscillation regime is established in several hundreds of picoseconds. This effect is naturally explained by the filling of a new coherent mode with the same $\mathbf{k} = \mathbf{k}_p = 0$ but different frequency. The oscillation period $T \approx 12$ ps approximately matches the inverse pump detuning $h/D \approx 10$ ps, which means that the new mode is located slightly above the ground polariton state.

The emergence of a new coherent polariton state with $\mathbf{k} = \mathbf{k}_p$ and $E < E_p$ is a very uncommon phenomenon. Being somewhat analogous to dynamical condensation [25], it is hardly expected under coherent driving, because such states cannot be excited via scattering from the pumped mode [33]. If $\mathbf{k}_p = 0$, the direct scattering leads only to the states with $\tilde{E}(\mathbf{k}) = E_p$, whereas all other two-particle processes are usually weak and do not reach the threshold of the parametric amplification. However, the abnormal population of scattered modes makes some of the indirect interaction channels particularly strong.

The diagram in Fig. 4(a) represents the interaction process resulting in the filling of the $k = 0$ mode near $E = E_g$. Specifically, each adjacent pair of the geometrically preferred states, e.g., $\mathbf{k}_1 = (\pm k_\star, 0)$ and $\mathbf{k}_2 = (0, \pm k_\star)$, scatters into $(0, 0)$ and $\mathbf{k}_1 + \mathbf{k}_2 = (\pm k_\star, \pm k_\star)$, which is consistent with energy conservation in the vicinity of the ground state where the polariton
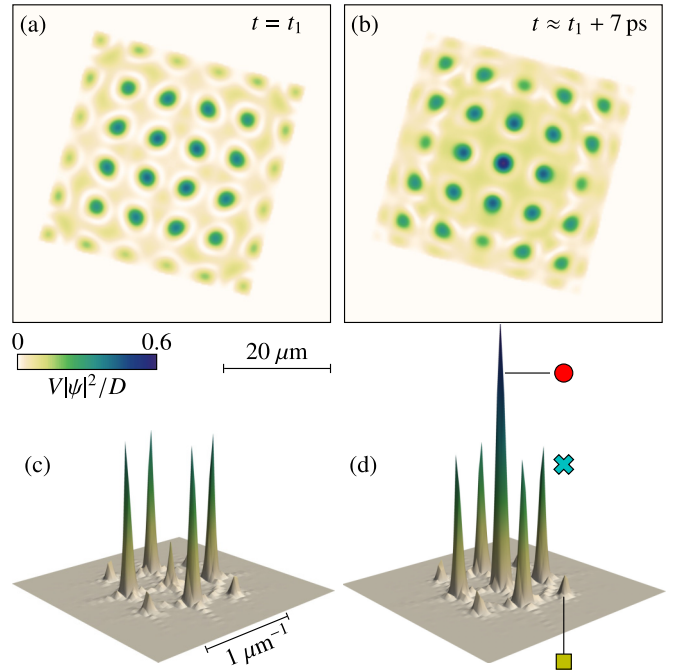

FIG. 5. Typical real-space [(a) and (b)] and momentum-space [(c) and (d)] field patterns at the stage of regular oscillations for two time instants separated by 7 ps (approximately half of a period). The full evolution can be seen in the Supplemental Material [34].

dispersion law is nearly parabolic. The overall scheme comprises a number of two-particle interactions; however, each of the $k_\star$ states acts as a source in two scattering processes at once, whereas the $k = 0$ state occurs as the joint target of all of them, which necessarily implies phase synchronization of different interaction channels.

Figures 4(b)–4(d) show the spectra of the main k states engaged in the loop scattering, which are obtained by the Fourier transform of $\psi_\mathbf{k}(t)$ over 2 ns at the stage of regular oscillations. As expected, the $k = 0$ state [Fig. 4(b)] has two peaks at $E = E_p$ and $E \gtrsim E_g$ whose intensities are nearly the same, in agreement with the fact that $I_p(t)$ drops down to zero at the oscillation minima. The geometrically preferred modes $k = k_\star$ [Fig. 4(c)] have, by contrast, only one strong peak at $E = E_p$ and thus appear to be particularly steady. The "idlers" with $k = \sqrt{2}k_\star$ [Fig. 4(d)] show the peak at $E \lesssim 2E_p - E_g$ whose total intensity (summed over four modes) nearly equals the intensity of the driven mode at $E = E_p$. Notice that all spectral lines are almost unbroadened, which is indicative of their "parametric" nature and precise synchronization of the respective k states. The spectra also contain sharp peaks near $(E - E_g)/D = 3, 4$, etc. (not shown); however, these peaks are located far from resonances and have thus comparatively low amplitudes.

The explicit real- and momentum-space distributions of $|\psi|^2$ are shown in Fig. 5 for two time instants which are nearly half a period apart; the corresponding continuous evolution is displayed in a separate video file [34]. It is seen that all modes in the k space except $k = 0$ remain nearly steady. Some of them are populated significantly; thus each change in ψ_0 has to be accompanied by a redistribution of $|\psi(\mathbf{r})|$ in the real

space in view of interference. As seen from comparison of Figs. 5(a) and 5(b), the growth of $I_p = |\psi_0|^2$ leads to a shift of the spatial lattice by nearly half of a period in both directions so that all maxima approximately turn into minima and vice versa. Notice as well that the maximum of $V|\psi(\mathbf{r}, t)|^2$, which is attained at the center of Fig. 5(b), is no greater than $0.6D$ and, therefore, the upper-branch states are not yet feasible even at a single point.

It is remarkable that rapid changes in I_p at the regular stage hardly affect I_s, which might seem untypical for a system with strong parametric instability of the pumped mode. The observed steadiness of I_s results in a constant rate of backscattering and, eventually, in a fully regular character of spatiotemporal oscillations. In its turn, it stems from the abnormal population: Since the pumped mode gives a comparatively small average contribution to the blueshift, I_s varies on the scale of the polariton lifetime $\tau = \hbar/\gamma$ that largely exceeds the oscillation period $T \gtrsim h/D$ as long as $\gamma \ll D$. The increase in $\langle I_p \rangle / \langle I_s \rangle$ would lead to an increased oscillation amplitude of I_s and, thus, increased volatility of the backscattering. As a result, the system experiences a transition to dynamical chaos. For the series of solutions represented in Fig. 2(a), this occurs in the last quarter of the middle branch, where ratio $\langle I_p \rangle / \langle I_s \rangle$ becomes nearly two times greater compared with the beginning of the same branch. Analysis of chaotic solutions is beyond the scope of this paper; we only notice that chaos makes the transition to the upper branch partially accidental, so that the two branches overlap within a finite range of pump powers around $0.5 f_\star^2$.

Turning back to self-pulsations, notice that the two main energy peaks of the $k = 0$ mode ($E = E_p$ and $E \approx E_g$) have equal intensities for most of the middle branch. Specifically, this is true in the range of f^2 from $0.2 f_\star^2$ (where that branch begins) to $0.4 f_\star^2$ (where the system experiences the first period-doubling bifurcation on its way to chaos). The equality of energy peaks and the corresponding full-scale oscillation of I_p are indicative of a precise balance of the direct and inverse scattering processes.

The length of the middle branch depends on the system size. The necessary condition of the considered phenomena is a strong inhomogeneity achieved already at $|f| \to 0$ owing to formation of standing waves. In other words, the geometrically preferred k states must be significantly stronger than all other modes with $k \neq 0$. This condition is met when the system size L is comparable to the distance traveled by the $k_\star$ polaritons on the scale of their lifetime. When that is the case, all k states become highly dissipative through multiple reflections from the potential walls, except for the "preferred" states which run perpendicular to one of them and form standing waves (generally speaking, this is true for all regular polygons of a reasonably small order). Thus an increase in the Q factor allows one to extend the range of the system sizes suitable to achieve the abnormal population and macroscopic loop scattering. The increase in Q also conforms to the other assumption that $\gamma \ll D$. It is worth noting that a state in which blueshift $V|\psi|^2 \sim D$ exceeds γ by more than ten times, with no side effects such as nonlinear losses, seems to be specific for polaritonic systems with strong exciton-photon coupling.

IV. DISCUSSION

To date, the parametric scattering of cavity polaritons is often thought to be just a macroscopic effect of the two-particle interaction with well-defined "source" and "target" k states. It was found, however, that for a greater D/γ the parametric scattering is an essentially collective process that successively involves many modes with different wave numbers $|\mathbf{k}|$ even when the pump amplitude is arbitrarily close to the threshold [22,23,33]. The most unstable many-mode states exhibit the abnormal population of scattered modes. As a rule, they are transient and only mediate the jump to the upper stability branch (for $k_p = 0$) or to a well-developed OPO regime with strong signal and idler modes. The aim of this work was to find a way to make the abnormal population persistent under constant driving conditions in a spatially extended polariton system. We have found it possible in the presence of a reduced rotational symmetry. The asymmetric (e.g., polygonal) systems show the macroscopic loop interaction in which several k states simultaneously act as the "sources" and "targets" of the parametric scattering.

The considered phase transition is somewhat analogous to the dynamical condensation [25]. Indeed, when the $k \neq 0$ modes, which are neither pumped nor energetically favored, acquire an abnormally high intensity, their multiple interactions result in the appearance of a new coherent mode near the ground-state level. The analogy with BECs or lasers is imperfect, however, because the new condensate is populated parametrically—in contrast to Ref. [25], where its formation has statistical reasons. At the same time, we have found the "condensation" to be accompanied by an induced synchronization of several backscattering channels, which is a relatively complex process that lies beyond the scope of plain two-particle interactions. The greater the polygon order, the greater the number of highly populated modes that become synchronized. Calculations show that even a purely circular shape of the microcavity does not prevent massive backscattering, which in this case proceeds through the spontaneous breakdown of the ring symmetry and results in chaotic dynamics. The statistical and, possibly, quantum aspects of the synchronized loop scattering have yet to be studied.

The self-pulsation of a polariton fluid under coherent driving is also a remarkable process that is usually prevented by the dissipative nature of polaritons combined with their interaction being of a purely repulsive kind (as opposed to lasers [35,36] and systems with self-focusing [37]). Even when the ground state is split into two spin or Josephson sublevels, both components of the condensate have the same "forced" energy E_p and thus do not oscillate at $|f| \to 0$ as well as $|f| \to \infty$. However, the combination of the ground-state splitting and nonlinearity does result in regular or chaotic oscillations in certain particular cases [26,27,38,39]. When V is nonzero and the spin splitting significantly exceeds γ, all one-mode states are forbidden in a finite range of $|f|$, resulting in chaos, dipolar networks, chimera states, and spontaneously formed vortices even for a purely uniform polariton system pumped by a plane wave [26,40,41]. These phenomena are underlain by a different kind of loop scattering that takes place in the presence of linear coupling of opposite spins [33,42]. By contrast, the system considered in this paper is effectively scalar, implying

that all polaritons have just the same spin, which corresponds to the case of circularly polarized excitation [43–46]. In contrast to another recent study, in which the second mode comes into play owing to size quantization in a micrometer-sized micropillar [27], our system has a large spatial extent, and the respective mode splitting is fairly negligible. Thus, the second condensate appears at $k = 0$ purely dynamically. Last, we notice that regular oscillations represent only the simplest kind of evolution, whereas the increase in $|f|$ or a more complex shape of microcavity result in new collective phenomena that call for investigation.

[1] C. Weisbuch, M. Nishioka, A. Ishikawa, and Y. Arakawa, Phys. Rev. Lett. **69**, 3314 (1992).

[2] Y. Yamamoto, T. Tassone, and H. Cao, *Semiconductor Cavity Quantum Electrodynamics* (Springer, Berlin, 2000).

[3] A. V. Kavokin, J. J. Baumberg, G. Malpuech, and P. Laussy, *Microcavities*, 2nd ed. (Oxford University Press, New York, 2017).

[4] J. Kasprzak, M. Richard, S. Kundermann, A. Baas, P. Jeambrun, J. M. J. Keeling, F. M. Marchetti, M. H. Szymańska, R. André, J. L. Staehli, V. Savona, P. B. Littlewood, B. Deveaud, and L. S. Dang, Nature (London) **443**, 409 (2006).

[5] A. Baas, J.-P. Karr, M. Romanelli, A. Bramati, and E. Giacobino, Phys. Rev. Lett. **96**, 176401 (2006).

[6] C. Ciuti, P. Schwendimann, and A. Quattropani, Semicond. Sci. Technol. **18**, S279 (2003).

[7] N. A. Gippius, S. G. Tikhodeev, V. D. Kulakovskii, D. N. Krizhanovskii, and A. I. Tartakovskii, Europhys. Lett. **67**, 997 (2004).

[8] I. Carusotto and C. Ciuti, Rev. Mod. Phys. **85**, 299 (2013).

[9] P. G. Savvidis, J. J. Baumberg, R. M. Stevenson, M. S. Skolnick, D. M. Whittaker, and J. S. Roberts, Phys. Rev. Lett. **84**, 1547 (2000).

[10] R. M. Stevenson, V. N. Astratov, M. S. Skolnick, D. M. Whittaker, M. Emam-Ismail, A. I. Tartakovskii, P. G. Savvidis, J. J. Baumberg, and J. S. Roberts, Phys. Rev. Lett. **85**, 3680 (2000).

[11] R. Butté, M. S. Skolnick, D. M. Whittaker, D. Bajoni, and J. S. Roberts, Phys. Rev. B **68**, 115325 (2003).

[12] D. M. Whittaker, Phys. Rev. B **63**, 193305 (2001).

[13] C. Ciuti, P. Schwendimann, and A. Quattropani, Phys. Rev. B **63**, 041303(R) (2001).

[14] G. Dagvadorj, J. M. Fellows, S. Matyjaśkiewicz, F. M. Marchetti, I. Carusotto, and M. H. Szymańska, Phys. Rev. X **5**, 041028 (2015).

[15] P. G. Savvidis, C. Ciuti, J. J. Baumberg, D. M. Whittaker, M. S. Skolnick, and J. S. Roberts, Phys. Rev. B **64**, 075311 (2001).

[16] D. M. Whittaker, Phys. Rev. B **71**, 115301 (2005).

[17] S. S. Gavrilov, N. A. Gippius, V. D. Kulakovskii, and S. G. Tikhodeev, J. Exp. Theor. Phys. **104**, 715 (2007).

[18] A. A. Demenev, A. A. Shchekin, A. V. Larionov, S. S. Gavrilov, V. D. Kulakovskii, N. A. Gippius, and S. G. Tikhodeev, Phys. Rev. Lett. **101**, 136401 (2008).

[19] D. N. Krizhanovskii, S. S. Gavrilov, A. P. D. Love, D. Sanvitto, N. A. Gippius, S. G. Tikhodeev, V. D. Kulakovskii, D. M. Whittaker, M. S. Skolnick, and J. S. Roberts, Phys. Rev. B **77**, 115336 (2008).

[20] M. Wouters and I. Carusotto, Phys. Rev. B **75**, 075332 (2007).

[21] K. Dunnett, A. Ferrier, A. Zamora, G. Dagvadorj, and M. H. Szymańska, Phys. Rev. B **98**, 165307 (2018).

[22] S. S. Gavrilov, Phys. Rev. B **90**, 205303 (2014).

[23] S. S. Gavrilov, A. S. Brichkin, Y. V. Grishina, C. Schneider, S. Höfling, and V. D. Kulakovskii, Phys. Rev. B **92**, 205312 (2015).

[24] C. E. Whittaker, B. Dzurnak, O. A. Egorov, G. Buonaiuto, P. M. Walker, E. Cancellieri, D. M. Whittaker, E. Clarke, S. S. Gavrilov, M. S. Skolnick, and D. N. Krizhanovskii, Phys. Rev. X **7**, 031033 (2017).

[25] C. Sun, S. Jia, C. Barsi, S. Rica, A. Picozzi, and J. W. Fleischer, Nat. Phys. **8**, 470 (2012).

[26] S. S. Gavrilov, Phys. Rev. B **94**, 195310 (2016).

[27] C. Leblanc, G. Malpuech, and D. D. Solnyshkov, Phys. Rev. B **101**, 115418 (2020).

[28] V. F. Elesin and Y. V. Kopaev, Zh. Eksp. Teor. Fiz. **63**, 1447 (1972) [Sov. Phys. JETP **36**, 767 (1973)].

[29] A. Baas, J. P. Karr, H. Eleuch, and E. Giacobino, Phys. Rev. A **69**, 023809 (2004).

[30] I. Carusotto and C. Ciuti, Phys. Rev. Lett. **93**, 166401 (2004).

[31] H. Haken, Rev. Mod. Phys. **47**, 67 (1975).

[32] M. J. Landman, G. C. Papanicolaou, C. Sulem, and P. L. Sulem, Phys. Rev. A **38**, 3837 (1988).

[33] S. S. Gavrilov, Phys.-Usp. **63**, 123 (2020).

[34] See Supplemental Material at http://link.aps.org/supplemental/10.1103/PhysRevB.103.184304 for a video file showing the real- and momentum-space dynamics of the system represented in Figs. 3–5.

[35] M. C. Cross and P. C. Hohenberg, Rev. Mod. Phys. **65**, 851 (1993).

[36] K. Staliunas and V. J. Sánchez-Morcillo, *Transverse Patterns in Nonlinear Optical Resonators* (Springer, New York, 2003).

[37] M. A. Ferré, M. G. Clerc, S. Coulibally, R. G. Rojas, and M. Tlidi, Eur. Phys. J. D **71**, 172 (2017).

[38] D. Sarchi, I. Carusotto, M. Wouters, and V. Savona, Phys. Rev. B **77**, 125324 (2008).

[39] D. D. Solnyshkov, R. Johne, I. A. Shelykh, and G. Malpuech, Phys. Rev. B **80**, 235303 (2009).

[40] S. S. Gavrilov, Phys. Rev. Lett. **120**, 033901 (2018).

[41] S. S. Gavrilov, Phys. Rev. B **102**, 104307 (2020).

[42] S. S. Gavrilov, JETP Lett. **105**, 200 (2017).

[43] I. A. Shelykh, A. V. Kavokin, Y. G. Rubo, T. C. H. Liew, and G. Malpuech, Semicond. Sci. Technol. **25**, 013001 (2010).

[44] M. Vladimirova, S. Cronenberger, D. Scalbert, K. V. Kavokin, A. Miard, A. Lemaître, J. Bloch, D. Solnyshkov, G. Malpuech, and A. V. Kavokin, Phys. Rev. B **82**, 075301 (2010).

[45] S. S. Gavrilov, A. S. Brichkin, A. A. Dorodnyi, S. G. Tikhodeev, N. A. Gippius, and V. D. Kulakovskii, JETP Lett. **92**, 171 (2010).

[46] A. V. Sekretenko, S. S. Gavrilov, and V. D. Kulakovskii, Phys. Rev. B **88**, 195302 (2013).